

## Title

# Terrestrial Organic Matter Amplifies Methane Emissions Across Sediments of the Mississippi River Headwaters

## Authors

Hailey M. Sauer<sub>1,2</sub>, Leslie A. Day<sub>1,3</sub>, Trinity L. Hamilton<sub>1,4</sub>\*

1. Department of Plant and Microbial Biology, University of Minnesota Twin Cities - St. Paul, MN, 55108 USA

2. St. Croix Watershed Research Station, Science Museum of Minnesota, Marine on St. Croix, MN, 55047 USA

3. Department of Microbiology and Immunology, Geisel School of Medicine at Dartmouth – Hanover, New Hampshire, 03755 USA

4. The BioTechnology Institute, University of Minnesota Twin Cities – St. Paul, MN, 55108  
USA

\* Corresponding Author

## Author Contribution Statement

HMS and TLH conceived the study and obtained the funds. HMS led fieldwork and microcosm set-up. HMS and LAD analyzed gas samples and HMS performed the data analysis and graphical representation of the results. HMS wrote the first draft of the manuscript, and all authors contributed significantly to the preparation of the final draft.

Trinity L. Hamilton | <https://orcid.org/0000-0002-2282-4655>  
[trinityh@umn.edu](mailto:trinityh@umn.edu)

Hailey M. Sauer | <https://orcid.org/0000-0001-6424-1047>

Leslie A. Day | <https://orcid.org/0000-0002-6330-3434>

34 **Scientific Significance Statement**

35 As human activities and climate change increase the amount of organic material entering lakes  
36 and rivers, understanding the effects this has on greenhouse gas emissions is crucial. Our study  
37 reveals that adding terrestrial organic matter to freshwater sediments universally boosts methane  
38 production, a potent greenhouse gas. Through the exploration of microbial communities  
39 responsible for this process, our research highlights how changes in terrestrial organic matter  
40 export to aquatic systems could increase methane emissions from sediments.

41

42 **Data Availability Statement**

43 Additional Supporting Information can be found in the online version of this article, including an  
44 extended version of methods and supplementary tables. Sequencing data associated with this  
45 paper is available on NCBI, BioProject PRJNA1164797.

46

47 **Abstract**

48 Terrestrial organic matter (tOM) plays a critical role in aquatic ecosystems, influencing carbon  
49 processes and greenhouse gas emissions. Here, we investigate the impact of tOM on methane  
50 production in littoral and pelagic sediments from the Mississippi River headwaters using a  
51 microcosm approach. Contrary to our expectations, tOM addition universally increased methane  
52 production across lentic sediments, with no significant difference between littoral and pelagic  
53 zones. Methane production was influenced by select sediment microorganisms, primarily  
54 methanogens and lignocellulose degrading bacteria, which responded similarly across different  
55 sediment habitats. The study highlights the role of cytochrome-containing methanogens and their  
56 syntrophic relationships with fermentative bacteria, emphasizing the significance of microbial  
57 community structure in sediment methane dynamics. Our findings suggest that increasing tOM  
58 loads to freshwater systems could have broader implications for methane emissions, driven by  
59 specific microbial interactions.

60

61 **Keywords**

62 Terrestrial Organic Matter (tOM), Methanogenic Archaea (Methanogens), Methane Production,  
63 Littoral, Pelagic, Sediment

64

65

66

67

68

69

70

71

## 72 **Introduction**

73 Terrestrial organic matter (tOM) plays a significant role in aquatic environments – influencing  
74 light, ecosystem metabolism, and food webs (Karlsson et al., 2009, 2012; Pace et al., 2004; Polis  
75 et al., 1997). Its role is not only pivotal in shaping the immediate environment but also holds  
76 significance in global carbon processes (Guillemette et al., 2017; Heathcote et al., 2015; Lapierre  
77 et al., 2013; Tittel et al., 2019; Wilkinson et al., 2013). Current global change scenarios predict  
78 an increase in the tOM load to lakes (Intergovernmental Panel On Climate Change (IPCC),  
79 2023). The effects of these changes on lake metabolism and carbon processes are uncertain  
80 (Karlsson et al., 2009, 2012; Pace et al., 2004; Polis et al., 1997) but may lead to increases in  
81 carbon emissions through terrestrial nutrient subsidies (Lapierre et al., 2013; Tittel et al., 2019).  
82 While both carbon dioxide (CO<sub>2</sub>) and methane (CH<sub>4</sub>) can be produced through tOM  
83 decomposition in lakes, anoxic CH<sub>4</sub> production in lake sediments is of particular interest given  
84 its higher warming potential (Grasset et al., 2018; IPCC 2023; Lapierre et al., 2013; Tittel et al.,  
85 2019).

86 Methane production by archaeal methanogenesis is strictly anaerobic and occurs predominantly  
87 in the sediments where oxygen is limited to the upper millimeters (Buan, 2018; Sobek et al.,  
88 2009). In these settings, methanogenic archaea (methanogens) can grow by reducing single  
89 carbon compounds (e.g., CO<sub>2</sub>, CO, methanol, methylamines) or acetate through one of several  
90 methanogenesis pathways (e.g., hydrogenotrophic, acetoclastic) (Buan, 2018). The use of  
91 simplified carbon compounds to fuel this reduction means methanogens are reliant upon other  
92 organisms to breakdown more complex organic matter (Liu & Whitman, 2008). As a result, the  
93 degradability of the organic matter and the structure of the microbial community equipped to  
94 degrade it strongly influences CH<sub>4</sub> production in sediments (Bastviken, 2009; West et al., 2012).

95 Several mechanisms influence microbial community assemblage (e.g., environmental filtering  
96 and stochastic processes), and within a lake there can be variation in microbial community size  
97 and structure – particularly between the littoral and pelagic zones (Cadotte & Tucker, 2017;  
98 Nemergut et al., 2011; Niño-García et al., 2016; Vincent et al., 2023). These differences arise in  
99 part due to the relative tOM load each of these zones receives (i.e., littoral > pelagic). As a result,  
100 CH<sub>4</sub> efflux from littoral sediments is often higher than that of the pelagic zone (Holgerson &  
101 Raymond, 2016). In experimental studies, tOM additions to littoral sediments have led to

102 increases in CH<sub>4</sub> production contradicting findings that tOM is not a significant contributor to  
103 carbon emissions (Grasset et al., 2018; Tittel et al., 2019; Yakimovich et al., 2020). This  
104 underscores the significance of OM loads to littoral sediments, while also examining variations  
105 in CH<sub>4</sub> production based on the source, be it terrestrial, phytoplankton, or aquatic macrophytes  
106 (Grasset et al., 2018). Considering the varied responses of sediments from a single lake basin to  
107 diverse OM sources, sediment regions might react differently due to their unique microbial  
108 community composition adapted to most efficiently degrade locally abundant OM compounds.  
109 Thus, a focus on sediment from one location leaves unexplored the potential differences in CH<sub>4</sub>  
110 responses to tOM across a lake basin with diverse microbial assemblages.

111 Here we aimed to assess the spatial heterogeneity of CH<sub>4</sub> production by pelagic, littoral, and  
112 riverine sediments as a response to tOM addition in a hydrologically connected system using a  
113 microcosm approach to better understand the biologic mechanisms underpinning observed  
114 differences in CH<sub>4</sub> production in aquatic systems. We expected that (a) CH<sub>4</sub> production rates  
115 would be higher in littoral than pelagic sediments due to a community structure more  
116 accustomed to degrading complex tOM, and that (b) variation in CH<sub>4</sub> production across the  
117 system would be related to the abundance and distribution of methanogenic communities.

118

## 119 **Materials and Methods**

### 120 *Study Site and Microcosm Design*

121 In June of 2020, we collected duplicate gravity cores from five sampling locations within the  
122 Mississippi River headwaters system (Fig 1A; Fig S1). Of these locations, two were pelagic, two  
123 were littoral, and one was riverine. Itasca State Park (Minnesota, USA) surrounds the system,  
124 and the watershed is predominately mature mixed deciduous and coniferous forest. We  
125 preformed loss on ignition (LOI) on a homogenized sample from 0-15cm for one core from  
126 every sampling location to determine the sediment organic fraction of each site (Table S1)  
127 (Dean, Jr., 1974). The remaining core for each site was used to set up microcosms with high,  
128 low, and no tOM (i.e., leaf litter) treatment groups. Detailed information regarding sampling  
129 locations (Table S1) and the set-up of the microcosms can be found in the supplemental  
130 information.

131

132 *Carbon to Nitrogen Ratios*

133 We measured total organic carbon (C), total organic nitrogen (N), and isotopic C and N ( $\delta^{13}\text{C}$ ,  
134  $\delta^{15}\text{N}$ ) on acidified (1M HCl for 24 hr) sediments pre and post microcosm using a Conflow IV  
135 open split interface connected to a Delta V Advantage IRMS (Table S2). We corrected the  
136 isotopic values using a set of known external standards including sucrose, GA40, and G41. We  
137 exhausted the remaining sample for each site and leaf litter and were unable to determine C and  
138 N in 2 samples: Pelagic B high tOM spike and leaf litter.

139

140 *Methane Concentrations*

141 During the incubation, we sampled the headspace gas for  $\text{CH}_4$  concentrations at days 1, 4, 7, 19,  
142 60, 90, 150, and 180 using a GC-2014 gas chromatograph. We converted these ppm  
143 concentrations to molar concentration using the ideal gas law and Henry's law, and we normalize  
144 production rates per gram C in the microcosm and reported as  $\mu\text{mol CH}_4 \text{ g}^{-1} \text{ d}^{-1}$  (Table S3).

145

146 *DNA Isolation, Sequencing, and Post-processing*

147 We isolated DNA from ~2g of sediment from the initial 0-15cm slurries for each location, ~6g of  
148 leaf litter, and ~2g of homogenized sediments from the three replicates for each tOM treatment  
149 microcosm post experiment. We sent DNA to the University of Minnesota Genomic Center for  
150 sequencing and targeted the V3-V4 hypervariable region of the 16S SSU rRNA using primers  
151 341F (5'- CCTAYGGGRBGCASCAG-3') and 806R (5'- GGACTACNNGGTATCTAAT-3')  
152 (Yu et al., 2005). We processed the resulting reads using Mothur (v.1.48.0) following the MiSeq  
153 SOP (Kozich et al., 2013; Schloss et al., 2009) and aligned our reads using the SILVA database  
154 (v.138) (Quast et al., 2013). We performed all subsequent analyses in R, including Latent  
155 Dirichlet Allocation (LDA) which correlates microbial communities with relevant environmental  
156 factors. A detailed description of LDA for microbiomes is provided in Sankaran and Holmes  
157 (2019) and also outlined in our SI methods (Sankaran & Holmes, 2019).

158

159 **Results and Discussion**

160 *Terrestrial OM additions increase methane production in lentic sediments*

161 The addition of tOM to sediments led to a significant increase in the production of  $\text{CH}_4$  across  
162 the 180-day experiment in all sampling locations (Fig 1B; Wilcoxon  $p < 0.01$ ). This increase in

163 CH<sub>4</sub> production came primarily from lentic sediments. There was no difference in CH<sub>4</sub>  
164 production between the pelagic and littoral sediment zones when tOM was added – contradicting  
165 our initial hypothesis that littoral sediments would produce more CH<sub>4</sub>. Unamended pelagic  
166 sediments produced more CH<sub>4</sub> than the other unamended sediment types (Fig 1C; Kruskal-Wallis  
167 & Dunn p<0.01). Sediments in Pelagic A and Pelagic B both had lower starting C:N ratios (~8;  
168 Table S1) which may explain greater CH<sub>4</sub> production in the control pelagic sediments. In  
169 previous studies, sediment C:N ratios less than 10 lead to greater CH<sub>4</sub> production regardless of  
170 sediment temperature (Duc et al., 2010). Pelagic sediments also receive less oxygen during the  
171 open water season and their starting microbial communities may have been more adapted to  
172 anoxic microcosm conditions.

173 Maximum CH<sub>4</sub> production occurred on day 1 in all lentic sediments (0.85 - 1.85  $\mu\text{mol CH}_4 \text{ g}^{-1}$   
174  $\text{d}^{-1}$ ). While it is possible the peak production on day 1 could be attributed to a rapid, positive  
175 priming effect (i.e., mineralization of organic C in the sediments stimulated by the addition of  
176 new material), we interpreted the high initial CH<sub>4</sub> concentrations to be from residual CH<sub>4</sub>  
177 diffused into the headspace during the microcosm setup. Previous research in similar OM  
178 amended microcosm studies, using both allochthonous and autochthonous C, support this  
179 assumption (Bertolet et al., 2022; Grasset et al., 2018). As a result, the statistics used to compare  
180 the overall data, sediment types, and sample sites do not include production from day 1.

181 After day 1, production decreased until day 19 when there was a secondary peak in basin A  
182 sediments (i.e., Littoral A1, Littoral A2, Pelagic A) (Fig 1D). We then saw production decrease  
183 until the end of the experiment when there was another, smaller, increase. The non-sinusoidal  
184 wave pattern observed in basin A sediments has also been observed in other microcosm studies  
185 looking at CH<sub>4</sub> production response due to tOM additions (Grasset et al., 2018). However, our  
186 observed rates are an order of magnitude lower. We attribute this difference to the prior study  
187 enriching sediments with nitrogen and phosphorous amended water. When comparing our results  
188 with microcosms that solely focus on the sediment microbes reaction to OM (autochthonously  
189 produced), we found similar CH<sub>4</sub> production.

190 The observed relationship between CH<sub>4</sub> production in response to tOM with added nutrients,  
191 combined with the correlation between trophic status and CH<sub>4</sub> production, underscores the  
192 possible co-limitation in the degradation of tOM and CH<sub>4</sub> production (Grasset et al., 2018; West

193 et al., 2016). This relationship is further accentuated when we differentiate samples based on  
194 their location. Basin A, a meso-eutrophic system, consistently shows higher average methane  
195 production across sediment types than basin B. Unfortunately, our study design omitted littoral  
196 sediments from basin B. Subsequent experiments could determine whether CH<sub>4</sub> production  
197 patterns (i.e., non-sinusoidal wave) maintain similar characteristics at a basin-level with equal  
198 representation of both littoral and pelagic sediments across basins.

199 Finally, we observed an increase in CH<sub>4</sub> across all river microcosms, including the control, after  
200 150 days (Fig 1D). While this response may have been a result of the initial river sediments  
201 adjusting to the anoxic conditions of the microcosm, we could not confidently determine this.  
202 Nevertheless, recent research has highlighted the importance of CH<sub>4</sub> production in rivers and  
203 streams – especially in agriculturally impacted systems (Berberich et al., 2020; Crawford et al.,  
204 2016; Stanley et al., 2016). We attributed the low CH<sub>4</sub> production observed in the riverine  
205 treatment condition to a low starting OM percentage (0.3% compared to ~20% in lentic  
206 sediments), and the lack of anthropogenic influence in the protected watershed.

207 *Sampling location is primary driver of microbial community composition*

208 We recovered 3135 OTUs belonging to 61 phyla across both archaeal and bacterial domains. We  
209 classified 67 OTUs as methanogens using taxonomy at the order level (Buan, 2018; Ou et al.,  
210 2022; Vanwonterghem et al., 2016). The most abundant OTU in the dataset was a methanogen,  
211 and there were 13 others in the top 100 – meaning methanogens are disproportionately abundant  
212 relative to their representation (only 2% of the 3135 total OTUs). Four of these OTUs, including  
213 the most abundant in the dataset, belong to acetoclastic *Methanosaeta* sp. or *Methanosarcina* sp.  
214 in the order Methanosarcinales. Members of Methanosarcinales contain cytochromes and have  
215 greater metabolic diversity (i.e., can grow on acetate, methylamines, H<sub>2</sub>) whereas all other known  
216 orders cannot use acetate for methanogenesis and are mainly characterized as hydrogenotrophs  
217 (using H<sub>2</sub> and/or formate to reduce CO<sub>2</sub>) (Lyu et al., 2018; Mand & Metcalf, 2019; Thauer et al.,  
218 2008).

219 Most freshwater CH<sub>4</sub> research focuses on categorizing methanogens based on methanogenesis  
220 pathways (i.e., acetoclastic vs. hydrogenotrophic). Here, we considered populations by the  
221 presence or absence of cytochromes to overcome limitations caused by multi-phyletic orders for  
222 hydrogenotrophic methanogens that differ in energy conservation strategies. By categorizing

methanogens this way, we attempted to understand population dynamics and potential nutrient cycling hot spots (Berberich et al., 2020; Biderre-Petit et al., 2019; Tardy et al., 2022). For example, selection for higher affinity to H<sub>2</sub> (non-cytochrome containing) would be advantageous when coexisting with sulfate reducers, which require higher concentrations of electron donors. Alternatively, possessing greater metabolic diversity (cytochrome containing) would facilitate persistence in the environment as available substrates fluctuate. Here, we found methanogens with and without cytochromes across all sediment types and sampling locations and there was no significant interaction between cytochrome status and treatment condition or location. Instead, the methanogen response appears to be a universal increase in abundance regardless of conservation strategy (Fig S2; Table S4). Although our study did not reveal clear niche differentiation based on energy conservation strategy, examining environmental methanogenic communities through the lens of cytochromes is a valuable approach for gaining a deeper understanding of population structure and nutrient dynamics and overcomes limitations and ambiguity inherent to categorizing by methanogenesis pathway.

Finally, and more broadly, we analyzed the structure of the methanogen communities across the sites and treatments using a principal component (PC) analysis (Fig 2A). The first two components explained 75.1% of the variance in the population, which differed based on sediment type (PERMANOVA R<sup>2</sup> 0.47; p<0.001) and sampling location (PERMANOVA R<sup>2</sup> 0.64; p<0.001). There is a large range in depth across the four lentic sampling locations (1.10–27.4m), and this significantly impacted community composition (Pearson R<sup>2</sup> 0.9868, p<0.001) (Berberich et al., 2020; Ruuskanen et al., 2018; Tardy et al., 2022; J. Zhang et al., 2015). Water column depth correlated with PC2, which explains 23.7% of the variation in community composition. While there were several OTUs that inform this component, there were four OTUs from the genus *Methanospirillum* which were highly abundant in the original sediment community of Basin B and increase in abundance following tOM enrichment – consistent with other experiments in lake and sewage sediments (Chen et al., 2020; Ward & Frea, 1980). In Chen et al. (2020), they found that the abundance of *Methanospirillum* was also significantly correlated with CH<sub>4</sub> and CO<sub>2</sub> production; however, the scores from our PC2 did not correlate with methane production rate.

252 Like the methanogen community, the entire bacterial and archaeal community differed based on  
253 sediment type (PERMANOVA  $R^2$  0.81,  $p < 0.001$ ) and sampling location (PERMANOVA  $R^2$   
254 0.69,  $p < 0.001$ ) (Fig 2B). Again, we found water depth to correlate with both PC1 and PC2  
255 (Pearson  $R^2$  0.54, 0.83 respectively) and the final C:N ratio from the microcosms was weakly  
256 correlated with PC2 (Pearson  $R^2$  0.38). However, the mean CH<sub>4</sub> production for sites and  
257 treatments showed no relationship with bacterial composition along either PC axis or final C:N  
258 ratio.

259 *Microbial sub-communities highlight complementary tOM degradation in sediments*

260 Our experimental microcosms showed that while sediment microbial communities differ by  
261 sampling location and sediment type, CH<sub>4</sub> production increased in response to tOM inputs  
262 irrespective of community. To further explore the role of unique microbial communities in  
263 different sampling locations and sediment types, we used LDA to fit our OTU data into sub-  
264 communities and looked for a significant differential abundance in those sub-communities across  
265 samples. We found several sub-communities to be differentially abundant when comparing  
266 sampling location. On average, sites had 20 significantly different sub-communities. However,  
267 low OTU-sub-community probability within made it such that we could not definitively describe  
268 patterns, as OTUs often overlap in both significant and insignificant sub-communities. In the  
269 pelagic sediments, nearly all sub-community were differentially abundant from river sediments;  
270 however, there were no significant sub-communities when comparing the littoral to the pelagic  
271 or river sediments.

272 When we compared these same sub-communities across tOM treatments, we found three (24, 25,  
273 & 31) to be differentially abundant given tOM addition (3 levels: Post-No, Post-Yes, Pre; Fig  
274 3A). Given the level order, all results are reported as a change from the Post-No treatment  
275 condition. We used a 1% cut off when determining the OTU-probabilities for each sub-  
276 community, resulting in a total of 46 OTUs that exhibit significant log<sub>2</sub> fold changes across the  
277 microcosm treatment. These 46 OTUs are members of eleven different phyla of which the top  
278 three are Firmicutes (15 OTUs), Proteobacteria (11 OTUs), and Bacteroidota (9 OTUs).  
279 Additionally, we found that between 50-80% of the differentially abundant sub-community  
280 OTUs are among the top 100 in terms of percent change (Fig 4). While all three of these sub-  
281 communities exhibit a strong and universal response to tOM additions, only sub-community 24

282 sample probabilities (i.e., gamma) correlated with our observed methane production rates  
283 (Pearson  $R^2$  0.324) (Fig 3B&3C).

284 Sub-community 24 had 19 OTUs and the greatest taxonomic diversity among the 3 differentially  
285 abundant sub-communities (8 phyla) (Fig 3D). Many of the OTUs in sub-community 24 were  
286 anaerobic microorganisms well adapted to the degradation of recalcitrant organic matter. For  
287 example, OTU00152 is a *Treponema* sp. of the family Spirochaetaceae and had the greatest sub-  
288 community-probability (~6%) – meaning it was more frequently associated with the sub-  
289 community structure. Members of the *Treponema* genus are noncellulolytic bacteria; however,  
290 they aid in the breakdown of cellulosic and lignin materials by interacting with lignocellulolytic  
291 bacteria like those in the families Prolixibacteraceae and Paludibacteraceae, both of which had  
292 multiple differentially abundant OTUs in sub-community 24 (Kudo et al., 1987; Leadbeater et  
293 al., 2021; Song et al., 2019). Both of these families, like many Bacteroidota, can secrete  
294 carbohydrate-active enzymes and have been linked with seasonal patterns of algal detritus  
295 degradation in glacial systems, and members of the family Prolixibacteraceae specifically have  
296 been shown to regulate the decomposition of aquatic plants in salt marshes (Leadbeater et al.,  
297 2021; Winkel et al., 2022). The degradation of cellulose in the environment is carried out by a  
298 consortia of bacteria that contain complementary enzymes enabling the complete breakdown of  
299 bulk tOM (Cragg et al., 2015). The bacterial consortia of sub-community 24 was found at all  
300 sampling locations and experienced significant shifts in abundance following the addition of  
301 tOM. Within sub-community 24, 15 of the 19 OTUs were among the top 100 shifting OTUs  
302 from pre to post microcosm (Fig 4).

303 In addition to seeing a clear signal response from the fermenting heterotrophic community to  
304 tOM treatment, we found two methanogens associated with distinct fermenting community  
305 structures – sub-community 24: *Methanosaeta* (OTU 00001) and sub-community 31:  
306 *Methanosaeta* (OTU00048). Both methanogens are members of the cytochrome containing  
307 order Methanosaetales and are commonly found in anaerobic digestor sludge where  
308 differences in the lipid or polysaccharide content of organic waste can affect the syntrophic  
309 partnerships (i.e., two organisms reliant on metabolic cooperation) – leading to different CH<sub>4</sub>  
310 yields (Chang et al., 2018; Kurade et al., 2019; Salama et al., 2019; J. Zhang et al., 2017). In  
311 these engineered systems, higher lipid content and syntrophic growth of Firmicutes with

312 *Methanosa* results in significantly higher CH<sub>4</sub> yields (Kurade et al., 2019; Saha et al.,  
313 2021). While our sub-community 31 illustrates this syntrophic relationship, the gamma-sample  
314 probabilities for sub-community 31 do not correlate with overall CH<sub>4</sub> production. This was due  
315 in part to the unique sample probability for Pelagic B basin with respect to this sub-community,  
316 and it potentially highlights that syntroph-methanogen relationships might be lake specific.  
317 Despite having low sub-community-OTU probabilities, as result of a relatively low sample size  
318 for this analysis (n=21), our LDA was able to uncover commonly occurring community  
319 structures like those of anaerobic digestor sludge and weakly correlate a single sub-community's  
320 OTU structure to increased CH<sub>4</sub> production. To assess the differential abundance of key taxa  
321 responsible for CH<sub>4</sub> production or other environmentally relevant byproducts, future studies  
322 could include a larger number of samples.

323 **Conclusion**

324 The mechanistic relationship between the structure of sediment microbial communities, OM, and  
325 CH<sub>4</sub> production is important to understand contrasting results observed in empirical studies.  
326 Here, we found similar patterns of CH<sub>4</sub> production in response to tOM and found a significant  
327 correlation between select hetero-fermentative bacteria in all sediments. We provide an  
328 alternative approach to examining methanogen population structures, one in which we consider  
329 energy conservation strategies (i.e., cytochrome-containing), and we find that the methanogens  
330 of this classification are strongly associated with tOM degrading OTUs in treatment conditions.  
331 Ultimately, our findings show that increased terrestrial production and subsequent tOM loads to  
332 lake sediments will have implications for lignocellulose degrading bacteria and subsequent CH<sub>4</sub>  
333 production by methanogenic archaea.

334

335 **Acknowledgements**

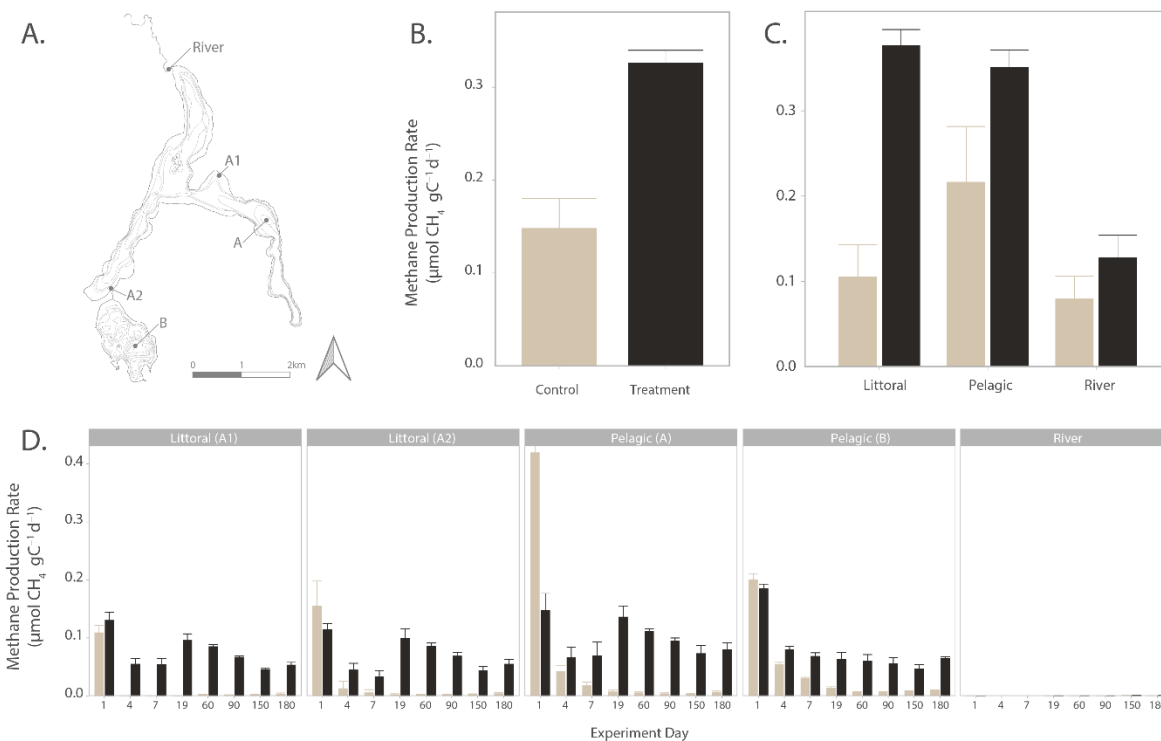
336 HMS and TLH acknowledge funding from NSF grant number 1948058. HMS thanks the Itasca Directors  
337 Fellowship for support. LAD thanks the MNDrive (UMII-GA-6798127534) for assistantship We are  
338 grateful to K. Fixen, N. Lewis, and J. Eggenberger for instrumentation and lab assistance.

339

340

341

342 **In Text Figure**

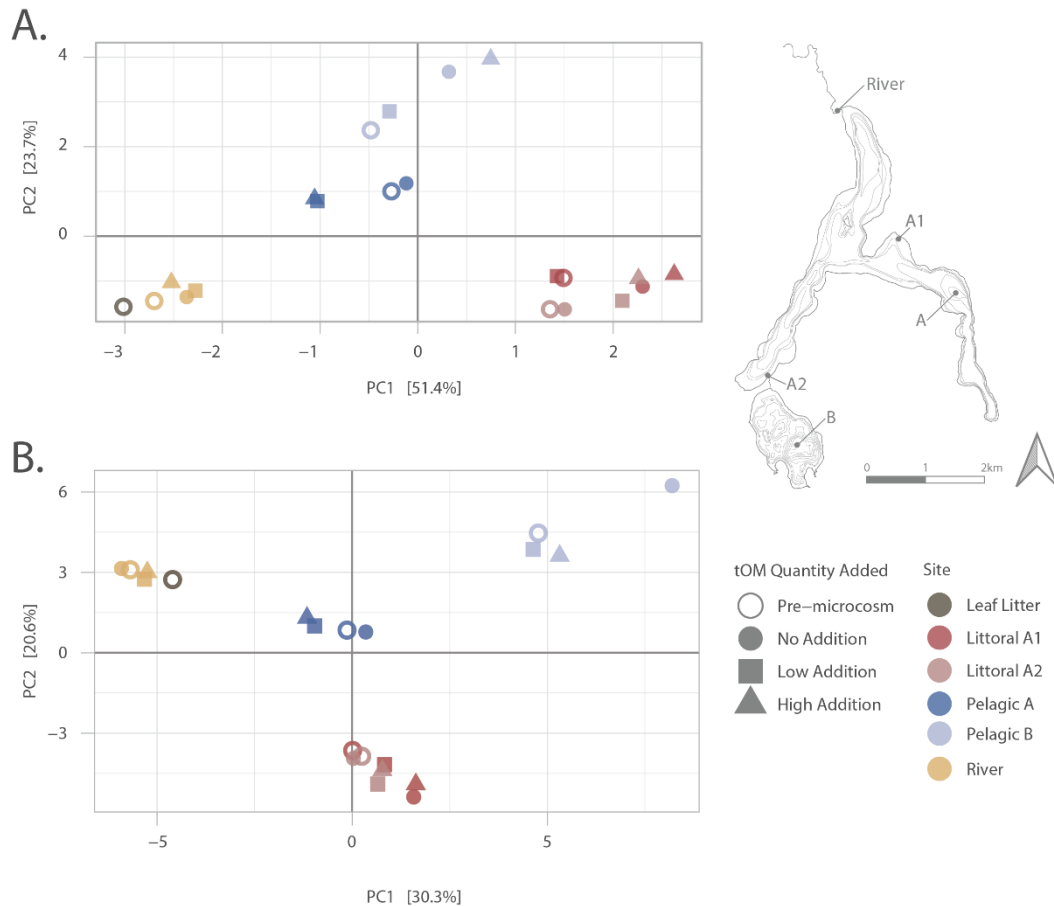


343

344 **Figure 1 – Methane production rates in response to terrestrial organic matter additions across**  
345 **different sediment types in the Mississippi River headwaters**

346 **A)** Bathymetric map (contour 10ft) showing spatial distribution of sampling locations within the  
347 Mississippi River headwaters, including littoral (A1, A2), pelagic (A, B), and River sites. **B)** Comparison  
348 of  $\text{CH}_4$  production rates ( $\mu\text{mol CH}_4 \text{ gC}^{-1} \text{ d}^{-1}$ ) between control (no tOM addition) and treatment (with  
349 tOM addition) conditions across all sediment types. There was a significant increase in  $\text{CH}_4$  production in  
350 the treatment group (Wilcoxon  $p<0.01$ ). **C)** Observed methane production rates ( $\mu\text{mol CH}_4 \text{ gC}^{-1} \text{ d}^{-1}$ )  
351 across different sediment types (Littoral, Pelagic, River) under treatment conditions. Both pelagic and  
352 littoral sediments exhibited higher methane production rates compared to river sediments, with no  
353 significant difference observed between the littoral and pelagic sediments (Kruskal-Wallis & Dunn  
354  $p<0.01$ ). **D)** Methane production rates ( $\mu\text{mol CH}_4 \text{ gC}^{-1} \text{ d}^{-1}$ ) for each sediment sampling location over the  
355 180-day incubation period (days 1, 4, 7, 19, 60, 90, 150, 180). The highest production rates were recorded  
356 on day 1, particularly in the pelagic A sediment, with rates subsequently decreasing until a secondary  
357 peak on day 19 in basin A sediments (Littoral A1, A2, Pelagic A). In all bar plots, the error bars are the  
358 standard deviation from the mean for the replicates.

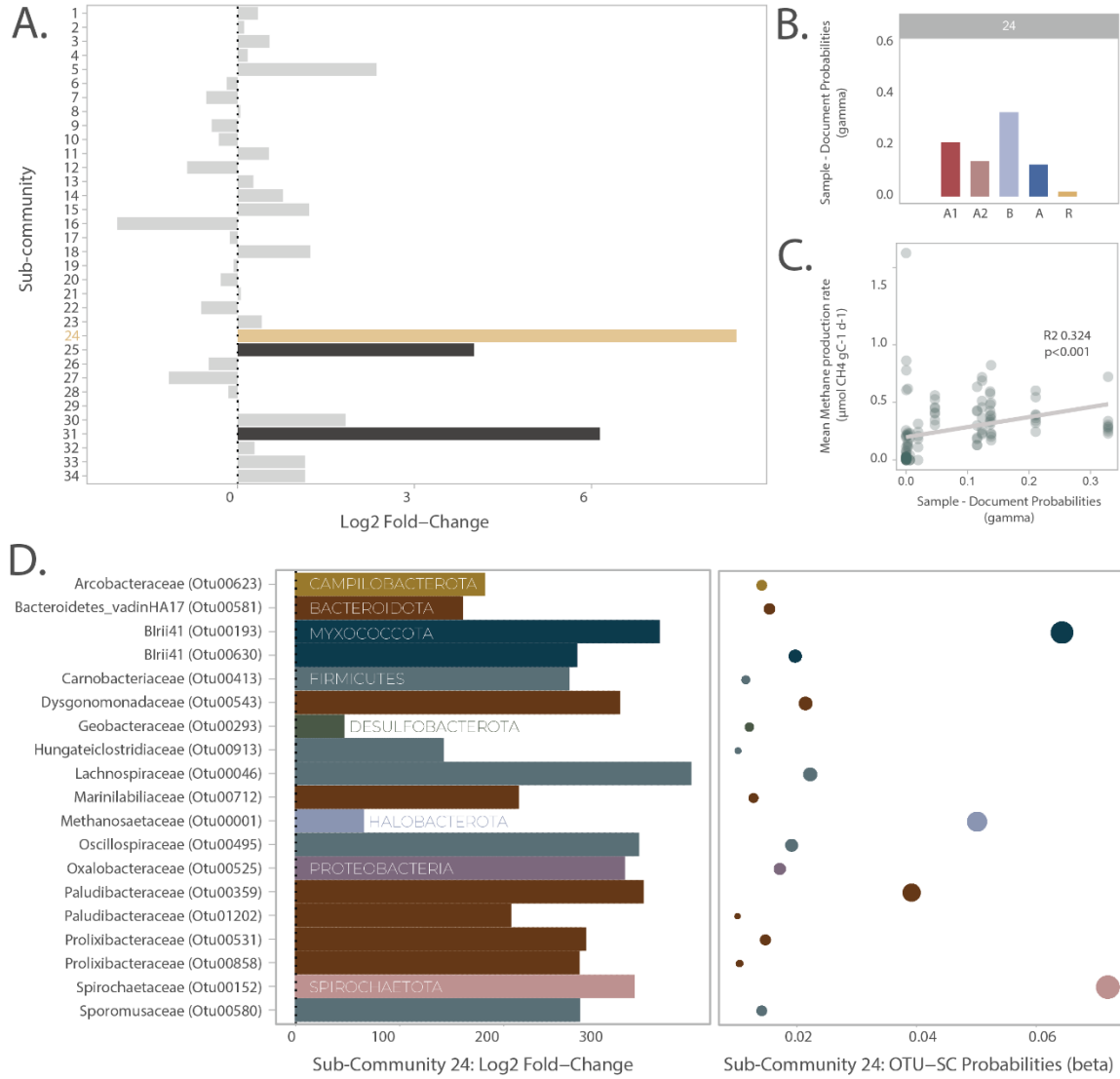
359



361 **Figure 2 – Principal component analysis (PCA) of microbial community composition in response to**  
362 **terrestrial organic matter (tOM) addition across sediment zones.**

363 A) PCA plot showing the first two principal components (PC1 and PC2) explaining 51.4% and 23.7% of  
364 the variance, respectively, in the methanogen community composition of sediments. The points represent  
365 different sampling sites (color) and treatment conditions (shape). Methanogen communities are primarily  
366 separated by sediment type (PERMANOVA  $R^2$  0.47;  $p<0.001$ ) and sampling location (PERMANOVA  $R^2$   
367 0.64;  $p<0.001$ ). Water column depth strongly correlates with PC2 (Pearson  $R^2$  0.9868,  $p<0.001$ ). B) PCA  
368 plot showing the first two principal components (PC1 and PC2) explaining 30.3% and 20.6% of the  
369 variance, respectively, in the entire microbial community. Sediment type (PERMANOVA  $R^2$  0.81,  
370  $p<0.001$ ) and sampling location (PERMANOVA  $R^2$  0.69,  $p<0.001$ ). The PCA suggest that sediment  
371 location is a selecting factor for community assemblage and that water column depth plays an important  
372 role in sorting these communities.

373



374

375 **Figure 3 – Latent Dirichlet Allocation Model | Microbial Sub-community response to terrestrial**  
 376 **organic matter (tOM) addition.**

377 A) Log2 fold-change in the abundance of 34 identified sub-communities following tOM addition across  
 378 sediment samples. Sub-communities 24, 25, and 31 showed significant differential abundance in response  
 379 to tOM addition, with sub-community 24 displaying the most substantial increase (log2 fold-change > 6)  
 380 and being the only sub-community correlated with increased CH<sub>4</sub> production. The x-axis represents the  
 381 magnitude of change, with positive values indicating an increase in abundance post-tOM addition. B)  
 382 Sample probabilities (gamma) for sub-community 24 across the sampling sites. The probabilities reflect  
 383 the association of sub-community 24 with specific sampling locations, with the highest probabilities  
 384 observed in Pelagic B and Littoral A1. C) Correlation between sample probabilities (gamma) for sub-

385 community 24 and mean CH<sub>4</sub> production rates (μmol CH<sub>4</sub> gC<sup>-1</sup> d<sup>-1</sup>). There is a significant positive  
386 correlation (R<sup>2</sup> = 0.324, p < 0.001), suggesting that the microorganisms in sub-community 24 may be  
387 linked to increased CH<sub>4</sub> production with respect to tOM addition. **D)** Taxonomic composition and OTU  
388 probabilities for sub-community 24. The bar plot on the left shows the log2 fold-change of key  
389 operational taxonomic units (OTUs) within sub-community 24, highlighting the predominant phyla,  
390 including Bacteroidota, Firmicutes, and Spirochaetota. The bubble plot on the right represents the OTU  
391 probabilities (beta) within sub-community 24, with larger bubbles indicating higher probabilities. OTUs  
392 such as *Treponema* sp. (family Spirochaetaceae) and members of the families Prolixibacteraceae and  
393 Paludibacteraceae are identified as key contributors to the degradation of recalcitrant organic matter in  
394 response to tOM. Color in both the left and right graph indicate the phylum of the OTU.

395

396

397

398

399

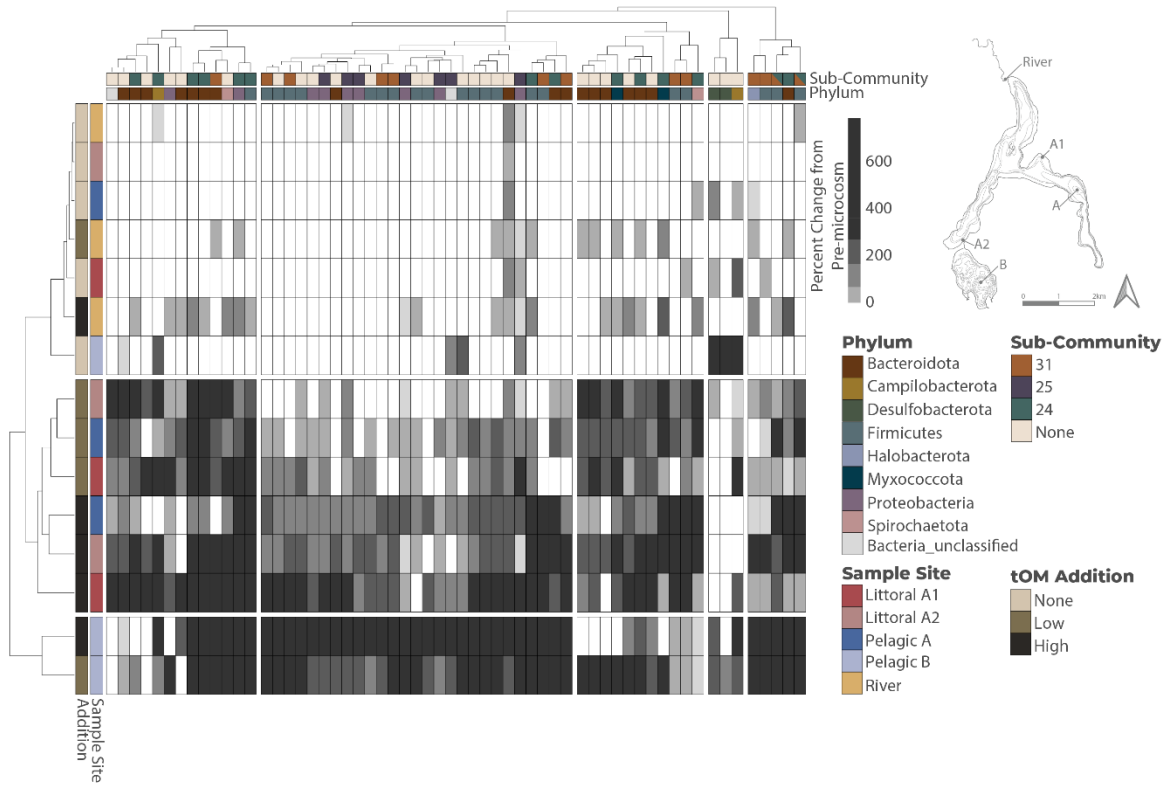
400

401

402

403

404



405

406

407 **Figure 4 – Percent Change of Top 100 OTUs from pre-microcosm to post-microcosm.**

408 Heatmap of percent change from pre-microcosm to post-microcosm. Columns represent the top 100  
409 changing OTUs and are Ward D2 clustered. Sub-community status is in the top box wherein the color  
410 represents presence within a specific sub-community – split colors indicate multiple sub-community  
411 presence. Each OTUs' phylum is then illustrated, also by color. Rows are Ward D2 clustered samples  
412 from the microcosms labeled by their sample location as well as tOM addition. Dendograms were split in  
413 the heatmap at n=3 for the rows and n=5 for the columns based on significant clusters (k-means). Within  
414 the top 100 OTUs microcosms cluster primarily by site and tOM status, where similar minimal change  
415 occurs in the OTUs with no tOM addition and in the river. Then there is a basin separation between those  
416 sites that are in basin A and those in basin B – specifically with respect to increases in OTUs belonging to  
417 sub-community 25 (purple) and those clustered with them in basin B.

418

419

420

421

422 **References**

423 Badri, M., Kurtz, Z. D., Müller, C. L., & Bonneau, R. (n.d.). *Normalization methods for microbial*  
424 *abundance data strongly affect correlation estimates*. 21.

425 Bastviken, D. (2009). Methane. In *Encyclopedia of Inland Waters* (pp. 783–805). Elsevier.  
426 <https://doi.org/10.1016/B978-012370626-3.00117-4>

427 Berberich, M. E., Beaulieu, J. J., Hamilton, T. L., Waldo, S., & Buffam, I. (2020). Spatial variability of  
428 sediment methane production and methanogen communities within a eutrophic reservoir:  
429 Importance of organic matter source and quantity. *Limnology and Oceanography*, 65(6), 1336–  
430 1358. <https://doi.org/10.1002/lno.11392>

431 Bertolet, B. L., Koepfli, C., & Jones, S. E. (2022). Lake Sediment Methane Responses to Organic Matter  
432 are Related to Microbial Community Composition in Experimental Microcosms. *Frontiers in*  
433 *Environmental Science*, 10. <https://www.frontiersin.org/article/10.3389/fenvs.2022.834829>

434 Biderre-Petit, C., Taib, N., Gardon, H., Hochart, C., & Debroas, D. (2019). New insights into the pelagic  
435 microorganisms involved in the methane cycle in the meromictic Lake Pavin through  
436 metagenomics. *FEMS Microbiology Ecology*, 95(3), fiy183.  
437 <https://doi.org/10.1093/femsec/fiy183>

438 Buan, N. R. (2018). Methanogens: Pushing the boundaries of biology. *Emerging Topics in Life Sciences*,  
439 2(4), 629–646. <https://doi.org/10.1042/ETLS20180031>

440 Cadotte, M. W., & Tucker, C. M. (2017). Should Environmental Filtering be Abandoned? *Trends in*  
441 *Ecology & Evolution*, 32(6), 429–437. <https://doi.org/10.1016/j.tree.2017.03.004>

442 Chang, S.-E., Saha, S., Kurade, M. B., Salama, E.-S., Chang, S. W., Jang, M., & Jeon, B.-H. (2018).  
443 Improvement of acidogenic fermentation using an acclimatized microbiome. *International*  
444 *Journal of Hydrogen Energy*, 43(49), 22126–22134.  
445 <https://doi.org/10.1016/j.ijhydene.2018.10.066>

446 Chen, H., Ye, J., Zhou, Y., Wang, Z., Jia, Q., Nie, Y., Li, L., Liu, H., & Benoit, G. (2020). Variations in  
447 CH4 and CO2 productions and emissions driven by pollution sources in municipal sewers: An

448 assessment of the role of dissolved organic matter components and microbiota. *Environmental*  
449 *Pollution*, 263, 114489. <https://doi.org/10.1016/j.envpol.2020.114489>

450 Cragg, S. M., Beckham, G. T., Bruce, N. C., Bugg, T. D., Distel, D. L., Dupree, P., Etxabe, A. G.,  
451 Goodell, B. S., Jellison, J., McGeehan, J. E., McQueen-Mason, S. J., Schnorr, K., Walton, P. H.,  
452 Watts, J. E., & Zimmer, M. (2015). Lignocellulose degradation mechanisms across the Tree of  
453 Life. *Current Opinion in Chemical Biology*, 29, 108–119.  
454 <https://doi.org/10.1016/j.cbpa.2015.10.018>

455 Crawford, J. T., Loken, L. C., Stanley, E. H., Stets, E. G., Dornblaser, M. M., & Striegl, R. G. (2016).  
456 Basin scale controls on CO<sub>2</sub> and CH<sub>4</sub> emissions from the Upper Mississippi River. *Geophysical*  
457 *Research Letters*, 43(5), 1973–1979. <https://doi.org/10.1002/2015GL067599>

458 Edgar, R. C., Haas, B. J., Clemente, J. C., Quince, C., & Knight, R. (2011). UCHIME improves  
459 sensitivity and speed of chimera detection. *Bioinformatics*, 27(16), 2194–2200.  
460 <https://doi.org/10.1093/bioinformatics/btr381>

461 Glassman, S. I., & Martiny, J. B. H. (2018). Broadscale Ecological Patterns Are Robust to Use of Exact  
462 Sequence Variants versus Operational Taxonomic Units. *mSphere*, 3(4).  
463 <https://doi.org/10.1128/mSphere.00148-18>

464 Gohl, D. M., Vangay, P., Garbe, J., MacLean, A., Hauge, A., Becker, A., Gould, T. J., Clayton, J. B.,  
465 Johnson, T. J., Hunter, R., Knights, D., & Beckman, K. B. (2016). Systematic improvement of  
466 amplicon marker gene methods for increased accuracy in microbiome studies. *Nature*  
467 *Biotechnology*, 34(9), 942–949. <https://doi.org/10.1038/nbt.3601>

468 Grasset, C., Mendonça, R., Villamor Saucedo, G., Bastviken, D., Roland, F., & Sobek, S. (2018). Large  
469 but variable methane production in anoxic freshwater sediment upon addition of allochthonous  
470 and autochthonous organic matter. *Limnology and Oceanography*, 63(4), 1488–1501.  
471 <https://doi.org/10.1002/lno.10786>

472 Grün, B., & Hornik, K. (2011). **topicmodels**: An R Package for Fitting Topic Models. *Journal of*  
473 *Statistical Software*, 40(13). <https://doi.org/10.18637/jss.v040.i13>

474 Guillemette, F., von Wachenfeldt, E., Kothawala, D. N., Bastviken, D., & Tranvik, L. J. (2017).  
475 Preferential sequestration of terrestrial organic matter in boreal lake sediments. *Journal of*  
476 *Geophysical Research: Biogeosciences*, 122(4), 863–874. <https://doi.org/10.1002/2016JG003735>

477 Heathcote, A. J., Anderson, N. J., Prairie, Y. T., Engstrom, D. R., & del Giorgio, P. A. (2015). Large  
478 increases in carbon burial in northern lakes during the Anthropocene. *Nature Communications*,  
479 6(1), Article 1. <https://doi.org/10.1038/ncomms10016>

480 Holgerson, M. A., & Raymond, P. A. (2016). Large contribution to inland water CO<sub>2</sub> and CH<sub>4</sub> emissions  
481 from very small ponds. *Nature Geoscience*, 9(3), Article 3. <https://doi.org/10.1038/ngeo2654>

482 Hornbach, D. J., Shea, K. L., Dosch, J. J., Thomas, C. L., Gartner, T. B., Aguilera, A. G., Anderson, L. J.,  
483 Geedey, K., Mankiewicz, C., Pohlad, B. R., & Schultz, R. E. (2021). Decomposition of Leaf  
484 Litter from Native and Nonnative Woody Plants in Terrestrial and Aquatic Systems in the Eastern  
485 and Upper Midwestern U.S.A. *The American Midland Naturalist*, 186(1), 51–75.  
486 <https://doi.org/10.1674/0003-0031-186.1.51>

487 Intergovernmental Panel On Climate Change (Ipcc). (2023). *Climate Change 2022 – Impacts, Adaptation*  
488 *and Vulnerability: Working Group II Contribution to the Sixth Assessment Report of the*  
489 *Intergovernmental Panel on Climate Change* (1st ed.). Cambridge University Press.  
490 <https://doi.org/10.1017/9781009325844>

491 Karlsson, J., Berggren, M., Ask, J., Byström, P., Jonsson, A., Laudon, H., & Jansson, M. (2012).  
492 Terrestrial organic matter support of lake food webs: Evidence from lake metabolism and stable  
493 hydrogen isotopes of consumers. *Limnology and Oceanography*, 57(4), 1042–1048.  
494 <https://doi.org/10.4319/lo.2012.57.4.1042>

495 Karlsson, J., Byström, P., Ask, J., Ask, P., Persson, L., & Jansson, M. (2009). Light limitation of nutrient-  
496 poor lake ecosystems. *Nature*, 460(7254), Article 7254. <https://doi.org/10.1038/nature08179>

497 Kolde, R. (2019). *Pheatmap: Pretty Heatmaps. R package version 1.0.12.* (Version v.1.0.12) [Computer  
498 software]. <https://CRAN.R-project.org/package=pheatmap>

499 Kozich, J. J., Westcott, S. L., Baxter, N. T., Highlander, S. K., & Schloss, P. D. (2013). Development of a  
500 dual-index sequencing strategy and curation pipeline for analyzing amplicon sequence data on the  
501 MiSeq Illumina sequencing platform. *Applied and Environmental Microbiology*, 79(17), 5112–  
502 5120. <https://doi.org/10.1128/AEM.01043-13>

503 Kudo, H., Cheng, K.-J., & Costerton, J. W. (1987). Interactions between *Treponema bryantii* and  
504 cellulolytic bacteria in the in vitro degradation of straw cellulose. *Canadian Journal of  
505 Microbiology*, 33(3), 244–248. <https://doi.org/10.1139/m87-041>

506 Kurade, M. B., Saha, S., Salama, E.-S., Patil, S. M., Govindwar, S. P., & Jeon, B.-H. (2019). Acetoclastic  
507 methanogenesis led by *Methanosarcina* in anaerobic co-digestion of fats, oil and grease for  
508 enhanced production of methane. *Bioresource Technology*, 272, 351–359.  
509 <https://doi.org/10.1016/j.biortech.2018.10.047>

510 Lapierre, J.-F., Guillemette, F., Berggren, M., & del Giorgio, P. A. (2013). Increases in terrestrially  
511 derived carbon stimulate organic carbon processing and CO<sub>2</sub> emissions in boreal aquatic  
512 ecosystems. *Nature Communications*, 4(1), Article 1. <https://doi.org/10.1038/ncomms3972>

513 Leadbeater, D. R., Oates, N. C., Bennett, J. P., Li, Y., Dowle, A. A., Taylor, J. D., Alponti, J. S.,  
514 Setchfield, A. T., Alessi, A. M., Helgason, T., McQueen-Mason, S. J., & Bruce, N. C. (2021).  
515 Mechanistic strategies of microbial communities regulating lignocellulose deconstruction in a UK  
516 salt marsh. *Microbiome*, 9, 48. <https://doi.org/10.1186/s40168-020-00964-0>

517 Love, M., Ahlmann-Eltze, C., Forbes, K., Anders, S., & Huber, W. (2020). *DESeq2: Differential gene  
518 expression analysis based on the negative binomial distribution* (Version 1.30.0) [Computer  
519 software]. Bioconductor version: Release (3.12). <https://doi.org/10.18129/B9.bioc.DESeq2>

520 Lyu, Z., Shao, N., Akinyemi, T., & Whitman, W. B. (2018). Methanogenesis. *Current Biology*, 28(13),  
521 R727–R732. <https://doi.org/10.1016/j.cub.2018.05.021>

522 Mand, T. D., & Metcalf, W. W. (2019). Energy Conservation and Hydrogenase Function in  
523 Methanogenic Archaea, in Particular the Genus *Methanosarcina*. *Microbiology and Molecular  
524 Biology Reviews: MMBR*, 83(4), e00020-19. <https://doi.org/10.1128/MMBR.00020-19>

525 McMurdie, P. J., & Holmes, S. (2013). phyloseq: An R Package for Reproducible Interactive Analysis  
526 and Graphics of Microbiome Census Data. *PLOS ONE*, 8(4), e61217.  
527 <https://doi.org/10.1371/journal.pone.0061217>

528 Nemergut, D. R., Costello, E. K., Hamady, M., Lozupone, C., Jiang, L., Schmidt, S. K., Fierer, N.,  
529 Townsend, A. R., Cleveland, C. C., Stanish, L., & Knight, R. (2011). Global patterns in the  
530 biogeography of bacterial taxa. *Environmental Microbiology*, 13(1), 135–144.  
531 <https://doi.org/10.1111/j.1462-2920.2010.02315.x>

532 Nikita, M. (2020). *ldatuning: Tuning of the Latent Dirichlet Allocation Models Parameters* (Version  
533 1.0.2) [Computer software]. <https://CRAN.R-project.org/package=ldatuning>

534 Niño-García, J. P., Ruiz-González, C., & del Giorgio, P. A. (2016). Interactions between hydrology and  
535 water chemistry shape bacterioplankton biogeography across boreal freshwater networks. *The  
536 ISME Journal*, 10(7), 1755–1766. <https://doi.org/10.1038/ismej.2015.226>

537 Oksanen, J., Kindt, R., Legendre, P., Hara, B., Simpson, G., Solymos, P., Henry, M., Stevens, H.,  
538 Maintainer, H., & Oksanen@oulu, jari. (2009). *The vegan Package*.

539 Ou, Y.-F., Dong, H.-P., McIlroy, S. J., Crowe, S. A., Hallam, S. J., Han, P., Kallmeyer, J., Simister, R. L.,  
540 Vuillemin, A., Leu, A. O., Liu, Z., Zheng, Y.-L., Sun, Q.-L., Liu, M., Tyson, G. W., & Hou, L.-J.  
541 (2022). Expanding the phylogenetic distribution of cytochrome b-containing methanogenic  
542 archaea sheds light on the evolution of methanogenesis. *The ISME Journal*, 16(10), Article 10.  
543 <https://doi.org/10.1038/s41396-022-01281-0>

544 Pace, M. L., Cole, J. J., Carpenter, S. R., Kitchell, J. F., Hodgson, J. R., Van de Bogert, M. C., Bade, D.  
545 L., Kritzberg, E. S., & Bastviken, D. (2004). Whole-lake carbon-13 additions reveal terrestrial  
546 support of aquatic food webs. *Nature*, 427(6971), Article 6971.  
547 <https://doi.org/10.1038/nature02227>

548 Polis, G. A., Anderson, W. B., & Holt, R. D. (1997). Toward an Integration of Landscape and Food Web  
549 Ecology: The Dynamics of Spatially Subsidized Food Webs. *Annual Review of Ecology and  
550 Systematics*, 28(1), 289–316. <https://doi.org/10.1146/annurev.ecolsys.28.1.289>

551 Quast, C., Pruesse, E., Yilmaz, P., Gerken, J., Schweer, T., Yarza, P., Peplies, J., & Glöckner, F. O.

552 (2013). The SILVA ribosomal RNA gene database project: Improved data processing and web-  
553 based tools. *Nucleic Acids Research*, 41(Database issue), D590–D596.

554 <https://doi.org/10.1093/nar/gks1219>

555 R Core Team. (2018). *R: A language and environment for statistical computing* [Computer software]. R  
556 Foundation for Statistical Computing. <https://www.R-project.org/>

557 Ruuskanen, M. O., St. Pierre, K. A., St. Louis, V. L., Aris-Brosou, S., & Poulain, A. J. (2018).  
558 Physicochemical Drivers of Microbial Community Structure in Sediments of Lake Hazen,  
559 Nunavut, Canada. *Frontiers in Microbiology*, 9.

560 <https://www.frontiersin.org/articles/10.3389/fmicb.2018.01138>

561 Saha, S., Kurade, M. B., Ha, G.-S., Lee, S. S., Roh, H.-S., Park, Y.-K., & Jeon, B.-H. (2021). Syntrophic  
562 metabolism facilitates Methanosaerina-led methanation in the anaerobic digestion of lipidic  
563 slaughterhouse waste. *Bioresource Technology*, 335, 125250.

564 <https://doi.org/10.1016/j.biortech.2021.125250>

565 Salama, E.-S., Saha, S., Kurade, M. B., Dev, S., Chang, S. W., & Jeon, B.-H. (2019). Recent trends in  
566 anaerobic co-digestion: Fat, oil, and grease (FOG) for enhanced biomethanation. *Progress in  
567 Energy and Combustion Science*, 70, 22–42. <https://doi.org/10.1016/j.pecs.2018.08.002>

568 Sankaran, K., & Holmes, S. P. (2019). Latent variable modeling for the microbiome. *Biostatistics*, 20(4),  
569 599–614. <https://doi.org/10.1093/biostatistics/kxy018>

570 Schloss, P. D., Westcott, S. L., Ryabin, T., Hall, J. R., Hartmann, M., Hollister, E. B., Lesniewski, R. A.,  
571 Oakley, B. B., Parks, D. H., Robinson, C. J., Sahl, J. W., Stres, B., Thallinger, G. G., Van Horn,  
572 D. J., & Weber, C. F. (2009). Introducing mothur: Open-Source, Platform-Independent,  
573 Community-Supported Software for Describing and Comparing Microbial Communities. *Applied  
574 and Environmental Microbiology*, 75(23), 7537–7541. <https://doi.org/10.1128/AEM.01541-09>

575 Sobek, S., Durisch-Kaiser, E., Zurbrügg, R., Wongfun, N., Wessels, M., Pasche, N., & Wehrli, B. (2009).  
576 Organic carbon burial efficiency in lake sediments controlled by oxygen exposure time and

577 sediment source. *Limnology and Oceanography*, 54(6), 2243–2254.

578 <https://doi.org/10.4319/lo.2009.54.6.2243>

579 Song, N., Xu, H., Yan, Z., Yang, T., Wang, C., & Jiang, H.-L. (2019). Improved lignin degradation

580 through distinct microbial community in subsurface sediments of one eutrophic lake. *Renewable*

581 *Energy*, 138, 861–869. <https://doi.org/10.1016/j.renene.2019.01.121>

582 Stackebrandt, E., & Goebel, B. M. (1994). Taxonomic Note: A Place for DNA-DNA Reassociation and

583 16S rRNA Sequence Analysis in the Present Species Definition in Bacteriology. *International*

584 *Journal of Systematic and Evolutionary Microbiology*, 44(4), 846–849.

585 <https://doi.org/10.1099/00207713-44-4-846>

586 Stanley, E. H., Casson, N. J., Christel, S. T., Crawford, J. T., Loken, L. C., & Oliver, S. K. (2016). The

587 ecology of methane in streams and rivers: Patterns, controls, and global significance. *Ecological*

588 *Monographs*, 86(2), 146–171. <https://doi.org/10.1890/15-1027>

589 Tardy, V., Etienne, D., Millet, L., & Lyautey, E. (2022). Lake Sediments From Littoral and Profundal

590 Zones are Heterogeneous but Equivalent Sources of Methane Produced by Distinct Methanogenic

591 Communities—A Case Study From Lake Remoray. *Journal of Geophysical Research: Biogeosciences*, 127(11), e2021JG006776. <https://doi.org/10.1029/2021JG006776>

593 Thauer, R. K., Kaster, A.-K., Seedorf, H., Buckel, W., & Hedderich, R. (2008). Methanogenic archaea:

594 Ecologically relevant differences in energy conservation. *Nature Reviews Microbiology*, 6(8),

595 Article 8. <https://doi.org/10.1038/nrmicro1931>

596 Tittel, J., Hüls, M., & Koschorreck, M. (2019). Terrestrial Vegetation Drives Methane Production in the

597 Sediments of two German Reservoirs. *Scientific Reports*, 9(1), Article 1.

598 <https://doi.org/10.1038/s41598-019-52288-1>

599 Vanwonterghem, I., Evans, P. N., Parks, D. H., Jensen, P. D., Woodcroft, B. J., Hugenholtz, P., & Tyson,

600 G. W. (2016). Methylotrophic methanogenesis discovered in the archaeal phylum

601 Verstraetarchaeota. *Nature Microbiology*, 1(12), Article 12.

602 <https://doi.org/10.1038/nmicrobiol.2016.170>

603 Vincent, W., Kumagai, M., & Couture, R.-M. (2023). *Wetzel's Limnology—Sediments and Microbiomes*  
604 (4th ed.).

605 Walter E. Dean, Jr. (1974). Determination of Carbonate and Organic Matter in Calcareous Sediments and  
606 Sedimentary Rocks by Loss on Ignition: Comparison With Other Methods. *SEPM Journal of*  
607 *Sedimentary Research*, Vol. 44. <https://doi.org/10.1306/74D729D2-2B21-11D7-8648000102C1865D>

608 Ward, T. E., & Frea, J. I. (1980). Sediment Distribution of Methanogenic Bacteria in Lake Erie and  
609 Cleveland Harbor. *Applied and Environmental Microbiology*, 39(3), 597–603.  
610 <https://doi.org/10.1128/aem.39.3.597-603.1980>

611 West, W. E., Coloso, J. J., & Jones, S. E. (2012). Effects of algal and terrestrial carbon on methane  
612 production rates and methanogen community structure in a temperate lake sediment. *Freshwater*  
613 *Biology*, 57(5), 949–955. <https://doi.org/10.1111/j.1365-2427.2012.02755.x>

614 West, W. E., Creamer, K. P., & Jones, S. E. (2016). Productivity and depth regulate lake contributions to  
615 atmospheric methane. *Limnology and Oceanography*, 61(S1), S51–S61.  
616 <https://doi.org/10.1002/lno.10247>

617 Wilkinson, G. M., Pace, M. L., & Cole, J. J. (2013). Terrestrial dominance of organic matter in north  
618 temperate lakes. *Global Biogeochemical Cycles*, 27(1), 43–51.  
619 <https://doi.org/10.1029/2012GB004453>

620 Winkel, M., Trivedi, C. B., Mourot, R., Bradley, J. A., Vieth-Hillebrand, A., & Benning, L. G. (2022).  
621 Seasonality of Glacial Snow and Ice Microbial Communities. *Frontiers in Microbiology*, 13.  
622 <https://www.frontiersin.org/articles/10.3389/fmicb.2022.876848>

623 Yakimovich, K. M., Orland, C., Emilson, E. J. S., Tanentzap, A. J., Basiliko, N., & Mykytczuk, N. C. S.  
624 (2020). Lake characteristics influence how methanogens in littoral sediments respond to  
625 terrestrial litter inputs. *The ISME Journal*. <https://doi.org/10.1038/s41396-020-0680-9>  
626

627 Yu, Y., Lee, C., Kim, J., & Hwang, S. (2005). Group-specific primer and probe sets to detect  
628 methanogenic communities using quantitative real-time polymerase chain reaction.  
629 *Biotechnology and Bioengineering*, 89(6), 670–679. <https://doi.org/10.1002/bit.20347>

630 Zhang, C. (2022). *MicrobiomeStat: Statistical Methods for Microbiome Compositional Data*. (Version  
631 1.1) [Computer software]. <<https://CRAN.R-project.org/package=MicrobiomeStat>>.

632 Zhang, J., Mao, L., Zhang, L., Loh, K.-C., Dai, Y., & Tong, Y. W. (2017). Metagenomic insight into the  
633 microbial networks and metabolic mechanism in anaerobic digesters for food waste by  
634 incorporating activated carbon. *Scientific Reports*, 7(1), Article 1. <https://doi.org/10.1038/s41598-017-11826-5>

635 Zhang, J., Yang, Y., Zhao, L., Li, Y., Xie, S., & Liu, Y. (2015). Distribution of sediment bacterial and  
636 archaeal communities in plateau freshwater lakes. *Applied Microbiology and Biotechnology*,  
637 99(7), 3291–3302. <https://doi.org/10.1007/s00253-014-6262-x>

638 Zhou, H., He, K., Chen, J., & Zhang, X. (2022). LinDA: linear models for differential abundance analysis  
639 of microbiome compositional data. *arXiv*. <https://arxiv.org/abs/2104.00242>

640

641

## 642 **Supplemental Methods**

### 643 *Microcosm Set-up*

644 We used the second core from each of the five sites for microcosms – following a 3x3 design  
645 with three tOM (dried leaf litter) treatments (0% tOM addition, 5% tOM addition, 15% tOM  
646 addition) each with three replicates. We extruded and homogenized the top 15cm of each core  
647 under micro-oxic conditions (using an inflatable anaerobic chamber filled with N<sub>2</sub>) and added the  
648 homogenized mixture to 125mL serum vials. We filled each vial to a depth of 2cm. For each  
649 core we filled the first three vials for the 0% tOM addition treatment and calculated the average  
650 sediment weight of the three replicates. We used this value and the starting sediment organic  
651 fraction percentage to determine the mass of dried leaf litter needed to increase the organic  
652 fraction by 5% and 15%. For tOM additions, we collected and homogenized a dried (105°C for  
653 12h; sieved through No. 5 mesh) mixture of leaves and needles from *Acer*, *Quercus*, and *Pinus*  
654 species. We assumed the leaf litter was 100% organic. While there was a statistically significant

655 difference in our tOM addition percentages between treatment (t-test;  $p<0.001$ ) there was overlap  
656 across the percentages and sites, as a result instead of referring to these as firm percentage  
657 additions we will refer to them as “low tOM spike” (target 5% tOM) and “high tOM spike”  
658 (target 15% tOM). To maintain anoxic conditions, we flushed all the vials with  $N_2$  before adding  
659 sediment and prior to sealing with a gas-tight butyl-rubber stopper and aluminum crimp. Finally,  
660 we covered the vials in tinfoil and stored them at 4°C in the dark for the duration of the  
661 experiment – 180 days. While we recognize that these conditions do not reflect the *in situ*  
662 conditions, our aim was to study methane production dynamics under consistent growth  
663 conditions, irrespective of the starting conditions of the initial sediment and abiotic forces.

664

#### 665 *Methane Concentrations*

666 We collected 10mL from the headspace of each vial using a gas-tight syringe and injected the  
667 sample into Labco Exetainers that were pre-flushed with helium. Exetainers were stored inverted  
668 at 4°C until they could be further processed. We replaced the microcosm headspace after every  
669 gas pull with 11mL  $N_2$  gas to maintain headspace pressure and avoid methanogenesis inhibition  
670 caused by the accumulation of  $CH_4$  or  $CO_2$  (Grasset et al., 2018). We measured  $CH_4$   
671 concentrations using a GC-2014 gas chromatograph equipped with a flame ionization detector  
672 and an 80/100 Porapak N column (6ft x 1/8in x 2.1mm SS). The carrier gas was argon run at a  
673 25mL  $min^{-1}$  flow rate, and the calibration standards ranged from 200 to 60,000ppm. We then  
674 converted these ppm concentrations to molar concentration using the ideal gas law and Henry’s  
675 law. All production rates reported in the text were normalized per gram of C in the microcosm  
676 and reported as  $\mu mol\ CH_4\ gC^{-1}\ d^{-1}$ . We used the values obtained from our total organic carbon  
677 analysis to normalize production rates by gram carbon in the supplemental materials. To  
678 calculate production rates per gram organic C OUT, we assumed the litter was 80% organic  
679 matter with a C:N ratio of 20 (Hornbach et al., 2021). Due to product backorders and shipping  
680 delays during the pandemic, we did not have enough Exetainers and were unable to pull gas  
681 samples from the Mississippi River site for days 4 and 7.

682

#### 683 *DNA Isolation, Sequencing, and Post-processing*

684 During the initial microcosm set up, we subsampled ~2g of sediment from the 0-15cm slurry and  
685 ~6g of leaf litter and stored these at -20°C until extraction. At the end of the experiment, we

686 combined and homogenized the sediment from the three replicates for each treatment. Again, we  
687 collected a ~2g from the pooled and homogenized sediment and stored it at -20°C until  
688 extraction. We extracted triplicate DNA for each sample using ~0.25g of sediment or leaf litter  
689 using a Qiagen Dneasy PowerSoil Pro kit following manufacturer protocols including 4°C  
690 incubation steps. We performed negative controls by carrying out extractions on blanks, using  
691 only reagents with no sample. We determined the final bulk DNA concentrations using a Qubit  
692 dsDNA HS Assay kit and Qubit Fluorometer. We did not detect any DNA in our blanks  
693 (detection limit for the assay kit is 10pg/µL). We then pooled 10µL of each DNA yielding  
694 replicate and recalculated bulk DNA for the pooled sample. We sent all DNA yielding samples  
695 and blanks to the University of Minnesota Genomic Center (UMGC) for sequencing.

696

697 The UMGC prepared libraries for the samples for Illumina sequencing using a Nextera XT  
698 workflow and 2x300bp chemistry. They targeted the V3-V4 hypervariable region of the bacterial  
699 and archaeal 16S SSU rRNA gene using primers 341F (5'- CCTAYGGGRBGCASCAG-3') and  
700 806R (5'- GGACTACNNGGTATCTAAT-3') (Yu et al., 2005). The amplicon preparation  
701 performed at the UMGC have been shown to be quantitatively more accurate and qualitatively  
702 complete than existing methods (Gohl et al., 2016). We recovered a total of 352,403 raw reads  
703 from 24 samples, including blanks and leaf litter. We processed these reads using Mothur  
704 (v.1.48.0) following the MiSeq SOP (Kozich et al., 2013; Schloss et al., 2009). We aligned our  
705 reads using the SILVA database (v.138) and removed chimeras with vsearch (v2.17.1) (Edgar et  
706 al., 2011; Quast et al., 2013). Finally, we classified the sequences as operational taxonomic units  
707 (OTUs) using a 97% similarity threshold and assigned taxonomy using the SILVA database  
708 (Glassman & Martiny, 2018; Stackebrandt & Goebel, 1994). After processing we had 273,151  
709 reads across the 24 samples.

710

711 All further analyses were conducted in R (v4.3.2) using the following packages: tidyverse,  
712 phyloseq, vegan, DESeq2, pheatmap, MicrobiomeStat, topicmodels, and ldatuning (Grün &  
713 Hornik, 2011; Kolde, 2019; Love et al., 2020; McMurdie & Holmes, 2013; Nikita, 2020;  
714 Oksanen et al., 2009; R Core Team, 2018; C. Zhang, 2022). Prior to analyzing the community  
715 composition of these sites, we filtered the data by removing any OTU that did not have 2 or more  
716 counts in at least 5% of samples. We also removed the nine OTUs which had reads in blank

717 samples, each OTU having a single read. After filtering, the average number of reads per sample  
718 was 13,762 and the minimum and maximum read depths were 8,858 and 20,302 respectively.  
719 OTU data have a strong positive skew due to many zero counts. To diminish these effects, we  
720 used a variance stabilizing transformation (Love et al., 2020). Log-like transformations such as  
721 this bring count data to near-normal distributions, produce larger eigengap values, and lead to  
722 more consistent correlation estimates all of which influence downstream analysis (Badri et al.,  
723 n.d.). To compare microbial community structure before and after the microcosm experiment, we  
724 conducted a principal component analysis (PCA) of the entire microbial community and the  
725 methanogen populations. From both PCAs we pulled the scores of the top two PCs and used  
726 those as variables for difference in composition when determining if sediment community  
727 composition influences CH<sub>4</sub> production. We determined methanogens based on taxonomy and  
728 compared the methanogen composition based on energy conservation strategies (i.e., those with  
729 or without cytochromes) (Buan, 2018; Ou et al., 2022; Thauer et al., 2008). Finally, we took two  
730 approaches to compare the change in populations from initial sediments to post-microcosm.  
731 First, we calculated the percent change in each OTU (after adding 10% the lowest observed pre-  
732 and-post microcosm abundance to any 0 values). We then selected the top 100 OTUs that had the  
733 greatest percent change from initial sediment to post-microcosm (eq. 1).

734

$$735 \frac{(postmicrocosmabundance + 0.0145) - (premicrocosmabundance + 0.0157)}{premicrocosmabundance + 0.0157}$$

736

737 Second, we used Latent Dirichlet Allocation (LDA) or topic modeling to examine the structural  
738 differences across microcosm treatments. LDA is a mixture model which correlates microbial  
739 communities with relevant environmental factors of interest. The advantages of using LDA over  
740 other mixed model approaches is that LDA allows fractional membership allowing samples to be  
741 composed of multiple sub-communities. The application of LDA models to microbiome datasets  
742 has been described in detail by Sankaran and Holmes 2019 (Sankaran & Holmes, 2019). Briefly,  
743 we determined the relevant number of topics or sub-communities (k=34) using the  
744 FindTopicsNumber function in ldatuning using a Gibbs sampling method and CaoJuan2009,  
745 Arun2010 metrics, and Deveaud2014. Then we conducted the LDA model again using Gibbs  
746 sampling and the topicsmodels package. We then converted our LDA model back to a phyloseq

747 object to further assess the differential abundance in the 34 sub-communities across select  
748 parameters (e.g., treatment addition, treatment quantity, and sample site). For this, we use the  
749 linda function in MicrobiomeStat with an alpha of 0.01, winsorization of outliers at 3%, and zero  
750 count data handling set to imputation – where in zero counts are given values with respect to  
751 sequencing depth (Zhou et al., 2022). From both approaches we aggregated the list of 100 most  
752 changed OTUs and those with >1% OUT-sub-community probabilities in the significantly  
753 different sub-communities (n=3; 46 OTUs) and evaluated how the abundances of those OTUs  
754 explained methane production rates.

755

756 **Supplemental Figures & Tables**

757 **Table S1 | Sampling Site Details**

758

759 **Table S2 | Carbon and Nitrogen Data**

760

761 **Table S3 | Methane Concentration & Production Rate Calculations**

762

763 **Table S4 | Cytochrome Status of Methanogens**

764

765

766

767

768

769

770

771

772

773

774

775

776

777

778

779

780

781

782

783

784

785

786

787 **Figure S1 | Map**

788 Bathymetric map (contour 10ft) showing spatial distribution of sampling locations within the Mississippi  
789 River headwaters, including littoral (A1, A2), pelagic (A, B), and River sites. Scale bar is for the  
790 bathymetric map. Elk Lake (basin B) and Lake Itasca (basin A) are the headwaters lakes of the  
791 Mississippi River located in Clearwater County, Minnesota USA.

792

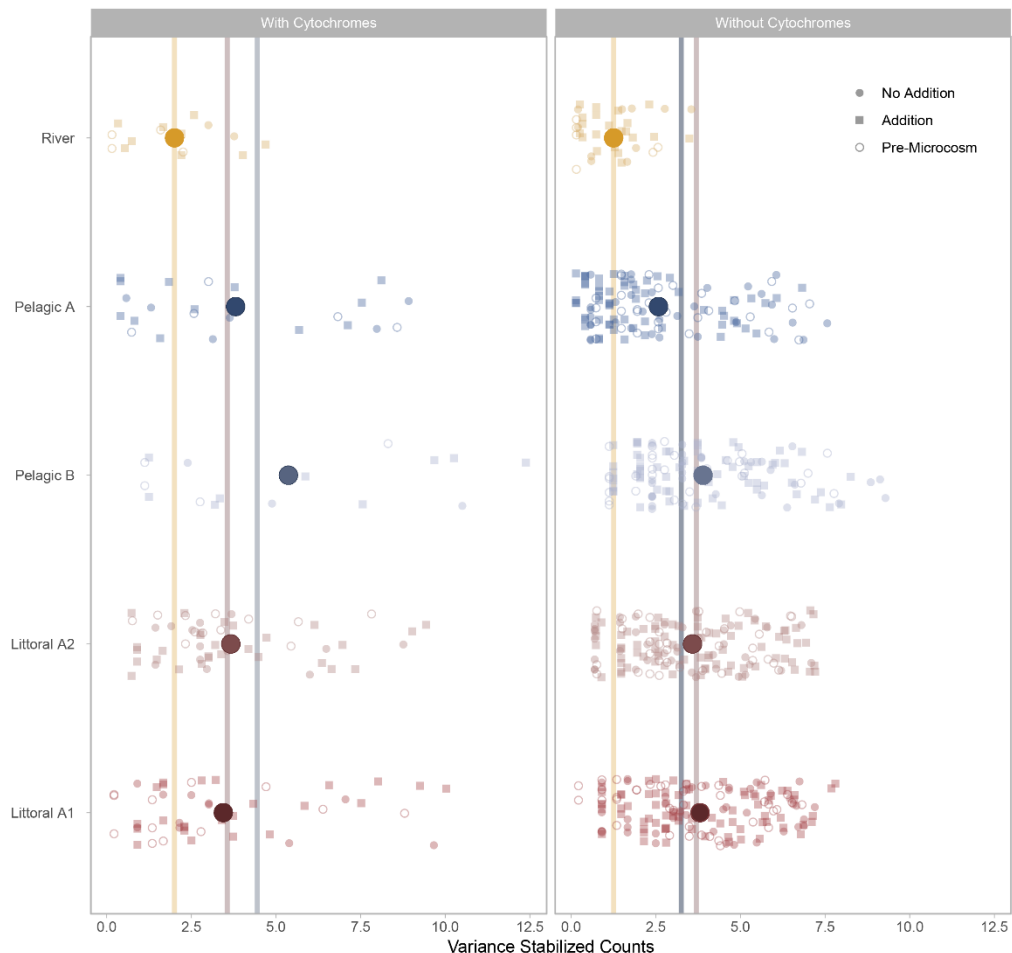


812

813 **Figure S2 | Methanogen Distribution**

814 The distribution of variance stabilized counts of methanogens with cytochromes (left) and  
815 without cytochromes (right). Each point is an OTU where color represents location and shape the  
816 microcosm status: pre-microcosm (empty circle), no addition (filled circle), and addition  
817 (square). Large circles are the average counts per site and lines are the average counts per  
818 sediment type: blue (pelagic) and red (littoral).

819



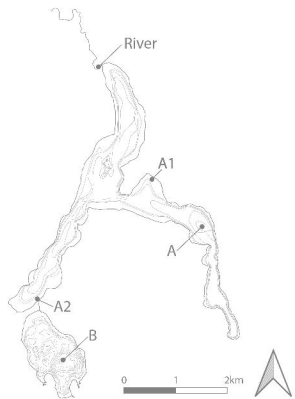
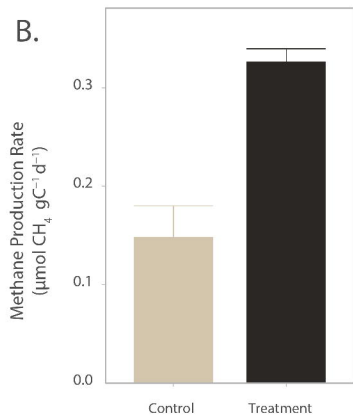
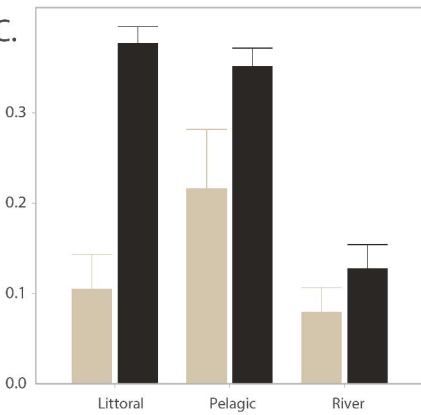
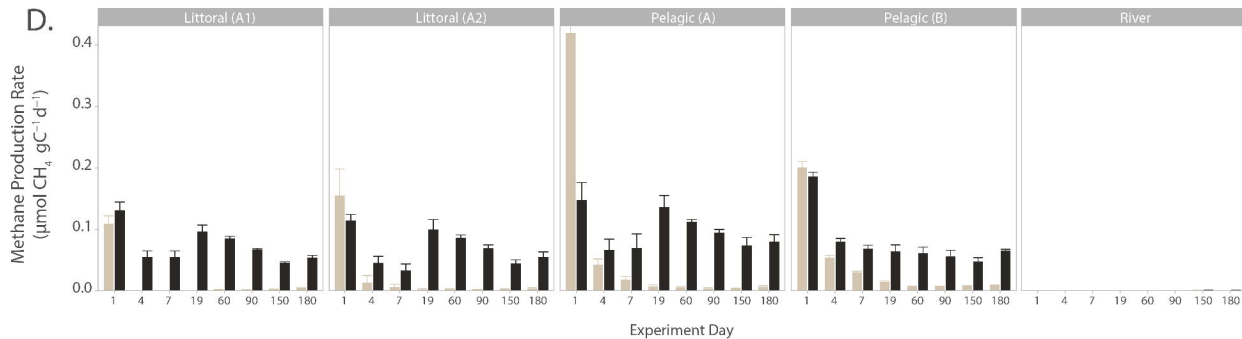
820

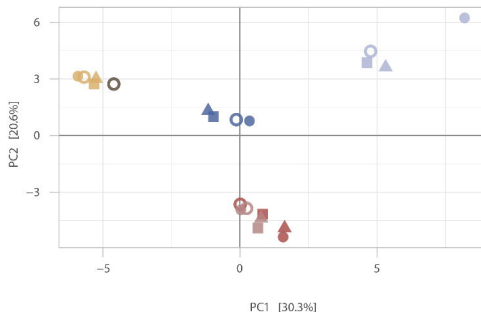
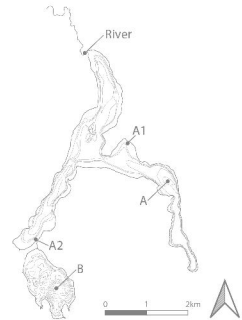
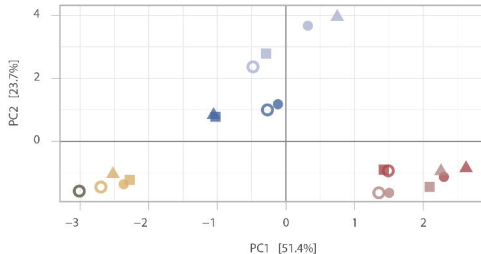
821

822

823

824

**A.****B.****C.****D.**



tOM Quantity Added	Site
Pre-microcosm	Leaf Litter
No Addition	Littoral A1
Low Addition	Littoral A2
High Addition	Pelagic A
Pre-microcosm	Pelagic B
River	River

